Solar Energy Materials & Solar Cells 103 (2012) 128–133

Contents lists available at SciVerse ScienceDirect

Solar Energy Materials & Solar Cells

journal homepage: www.elsevier.com/locate/solmat

Variable light biasing method to measure component I–V characteristics of multi-junction solar cells

J. Holovský [a,b,*], M. Bonnet-Eymard [a], M. Boccard [a], M. Despeisse [a], C. Ballif [a]

[a] Ecole Polytechnique Fédérale de Lausanne (EPFL), Institute of Micro-engineering (IMT), Photovoltaics and Thin-film Electronics Laboratory, Rue Breguet 2, 2000 Neuchatel, Switzerland

[b] Institute of Physics of the ASCR v. v. i., Cukrovarnicka 10, 162 53 Prague 6, Czech Republic

ARTICLE INFO

Article history:
Received 23 February 2012
Received in revised form
3 April 2012
Accepted 10 April 2012
Available online 9 May 2012

Keywords:
Current–voltage characteristics
Multi-junction
P–i–n
Light bias

ABSTRACT

We present a new technique to measure component current–voltage (I–V) curves of individual sub-cells integrated in a monolithic multi-junction solar cell. This new approach, compared to all previously reported ones, is well suited for thin-film silicon p–i–n structures where the so-called shifting approximation, which supposes that illumination only shifts the I–V curve without changing its shape, is not valid. Moreover, the proposed method is particularly resistant to problems related to electrical shunts. The principle of this method lies in coupling the level of a selective light bias with the level of measured electrical current in order to fix the voltage of a selected sub-cell while sweeping over the current axis. When one of the sub-cells has a fixed voltage, it is then possible to get the I–V characteristics of the second one, shifted by a fixed voltage value. This measurement procedure is simple and requires no modeling. The accuracy of the method is evaluated by numerical simulations of a thin-film silicon p–i–n photodiode. Our technique is then successfully experimentally tested on a specially prepared three-terminal amorphous/microcrystalline silicon tandem solar cell.

1. Introduction

The multi-junction structure is a proven way to increase device efficiency in many solar cell technologies. In the thin-film silicon technology, one of the most common approaches is to combine an amorphous (a-Si:H) silicon cell and a microcrystalline (μc-Si:H) silicon cell into a so-called micromorph tandem solar cell structure [1]. The advantage of such a structure is the ability to absorb more efficiently a larger part of the solar spectrum by stacking materials with different bandgaps. For cell and module diagnostics, both in research and production, the current–voltage (I–V) measurement is the most common characterization tool. However, due to the monolithic integration of the two sub-cells, only measurements of the multi-junction's overall I–V are currently common. Although many I–V separation methods have already been reported [2–9], due to their complexity or limitations, none of them has become a standardized method of evaluation of the I–V performance of separate sub-cells in multi-junction devices. In this article we introduce a new and promising technique.

1.1. Effect of illumination

A common approach in the variety of reported methods [2–9] is the application of additional selective illumination. Indeed, the sub-cells are sensitive to different parts of the light spectrum. Thus, using selective illumination is the only non-destructive way of accessing individual sub-cells. In this part we first analyze theoretically the effect of the illumination on p–i–n solar cell I–V characteristics.

In the simplest model, the electrical performance of the solar cell can be described by Eq. (1) that takes into account the diode behavior, the parasitic serial resistance R_s and the shunt resistance R_{sh}. The symbols I, V, I_{ph}, I_s, n, k, and T respectively correspond to current and voltage on terminals, photogenerated current, saturation current, ideality factor, Boltzmann constant, and temperature:

$$I = -I_{ph} + I_s\left(\exp\left(\frac{V - IR_s}{nkT}\right) - 1\right) + \frac{V - IR_s}{R_{sh}} \tag{1}$$

The simplified assumption that the illuminated I–V characteristic is equivalent to the dark I–V ($I_{ph}=0$) shifted by the photogeneration I_{ph} along the vertical axis, called the shifting approximation [10], is valid only under restricted conditions. As shown already by Wolf and Rauschenbach [11], this assumption is violated by the presence of serial resistance R_s that introduces the current I also to the right side of Eq. (1). Apart from this effect of

* Corresponding author at: Institute of Physics of the ASCR v. v. i., Cukrovarnicka 10, 162 53 Prague 6, Czech Republic. Tel.: +420 220 318 516; fax: +420 233 343 184.
E-mail addresses: j.holovsky@gmail.com (J. Holovský), max.bonnet-eymard@epfl.ch (M. Bonnet-Eymard), mathieu.boccard@epfl.ch (M. Boccard), matthieu.despeisse@epfl.ch (M. Despeisse), christophe.ballif@epfl.ch (C. Ballif).

0927-0248/$ - see front matter © 2012 Elsevier B.V. All rights reserved.
http://dx.doi.org/10.1016/j.solmat.2012.04.014

the serial resistance, the shifting approximation has been attributed to the superposition principle of solving linear differential equations and has been critically analyzed for p–n junction solar cells [10,12]. Even in the case of crystalline silicon solar cells, the introduction of processes such as surface recombination can invalidate the shifting approximation. For thin-film p–i–n junctions, this approximation has been dismissed for both empirical [13] and fundamental reasons (presence of amphoteric recombination centers in the i-layer). This is expressed in Merten's model [14] by the addition of a new voltage-dependent recombination term I_{rec} (2) to the right side of Eq. (1):

$$I_{rec} = I_{ph}\frac{d^2}{(\mu\tau)_{eff}(V_{bi} - V + IR_s)} \tag{2}$$

Here, d, $(\mu\tau)_{eff}$, and V_{bi} indicate the thickness of the intrinsic layer, the effective mobility–lifetime product, and the built-in potential, respectively. We present a method that does not depend on the shifting approximation directly, thus significantly reducing the error.

By recording the evolution of the short-circuit current (I_{SC}) versus the open-circuit voltage (V_{OC}) when going from dark to full illumination, the so-called pseudo-*I–V* curve [11,15] can be obtained. For p–n junctions, such a curve is often interpreted as approximately the dark *I–V* of the given cell, but without the effect of serial resistance R_s. The exact difference between the pseudo and dark *I–V* curves in p–n junctions is now being considered as more complex [16]. Again, for thin-film silicon p–i–n structures, such an interpretation would mean an even poorer approximation, because of the presence of the recombination term (2). From this brief overview we can conclude that any measurement technique giving an illuminated *I–V* curve must be—in the case of thin-film p-i-n silicon cells—also performed at this illumination.

The explanation of the effect of illumination on the *I–V* curve of a multi-junction solar cell relates to the analysis of individual operating points of the individual sub-cells [11]. At any condition, the operation of any sub-cell is fully defined by the (operating) point that lies on its respective *I–V* curve and that fulfills all additional physical conditions. Thus the operating points of cells connected in series must be at the same current. The total voltage is then the sum of the voltages of all points. The selective illumination of one sub-cell can shift its respective *I–V* curve, while the vertical position of the operating point will still be determined by the level of the common electrical current. Voltage as a function of current will be a sum of voltages of two operating points lying at the same current level (see Fig. 1).

1.2. State of the art

Several *I–V* separation methods aim at measuring the *I–V* characteristics of one sub-cell by fixing the voltages of the other ones. Fixing the voltage of a given sub-cell can be done by using a constant selective light bias [2–4] that shifts its respective *I–V* characteristic downward and, since the operating point must stay at the same current, it will be moved along the *I–V* curve and can be moved to its steep part. If the slope of the steep part (its lower bound corresponds to R_{OC}^{-1}, defined e.g. in [14]) is high enough, the voltage on the illuminated sub-cell can be assumed to be constant. In Fig. 1, the effect of light biasing on the bottom sub-cell of a tandem cell is shown. The lowest lying red curve corresponds to the constant light bias method. When the *I–V* curve of the device is then measured, the voltage contribution of the light-biased sub-cell corresponds to the V_{OC} plus a variation given by the slope of its *I–V* curve (see the trajectories of the operating points denoted by black circles and dashed lines in Fig. 1). To obtain the component *I–V* curve, this voltage contribution has to be subtracted. Either a value of V_{OC} is simply assumed [2,4] or a default shape is used [3]. In order to take into account the real shape of the voltage variation, some more advanced methods that use several intensity levels of constant light bias exist. However, a complex mathematical analysis that is again based on the shifting approximation has to be used to recover the component *I–V* curves [5,7] or their basic parameters [6]. Determining a sub-cell's individual V_{OC} is a specific problem of some of the latter methods. In some of them [4–6,9] the V_{OC} is obtained directly from the method; however in other ones [2,3,7] it is a necessary input.

Another possibility is to perform spectrally selective suns–V_{OC} measurements [15] to obtain separate pseudo-*I–V* curves for individual sub-cells [8,9]. V_{OC} is measured by applying selective illumination with intensity varying from dark to the equivalent of 1 sun. The current is calculated from the sub-cell's I_{SC} at 1 sun, measured by the integral of the external quantum efficiency (*EQE*) and from the assumption of its linear dependence on intensity [15]. As discussed before, pseudo-*I–V* curves are difficult to be interpreted as illuminated *I–V* characteristics. Nevertheless this method can still be useful for obtaining V_{OC} because both pseudo-*I–V* and illuminated *I–V* curves go through the same V_{OC} point [11]. However, this approach requires perfectly selective illumination because even a very small parasitic generation in an unbiased sub-cell can vastly corrupt the results. We recently developed an algorithm to obtain reliable V_{OC} values for

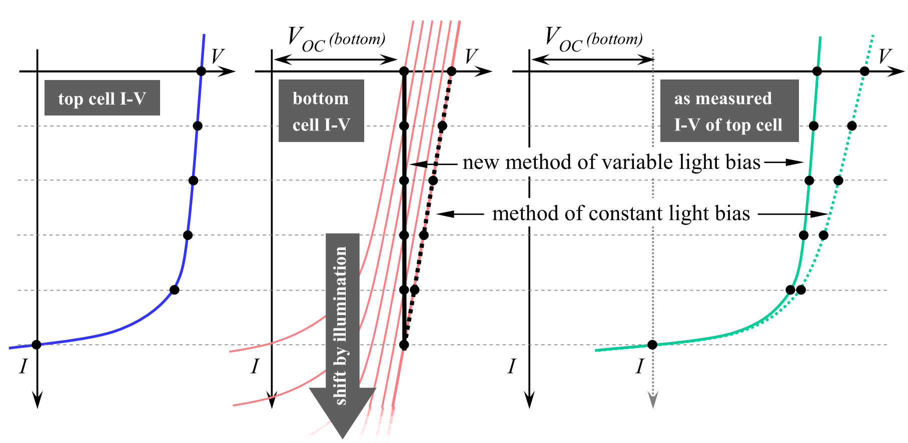

Fig. 1. Measured *I–V* curves (on the right) as a product of summation in voltage domain of the top cell voltage (on the left) and the voltage of the light biased bottom cell (in the middle). Light bias shifts the *I–V* curve vertically. Dotted lines represent attempt to eliminate the variation of voltage on the bottom cell by vertical shift of its *I–V* curve due to a constant light bias. Full lines represent new method of a variable light bias where the vertical shift scales with the level of current. (For interpretation of the references to color in this figure, the reader is referred to the web version of this article.).

individual sub-cells even in cases of imperfect selectivity of light bias [17]. In the paper presented here we will suppose that the sub-cell's individual V_{OCs} can be obtained by this method.

2. Experiment

2.1. Principle

As discussed, the constant light biasing method is affected by the additional voltage variation given by the slope of the steep part of the I–V characteristic of the non-evaluated sub-cell(s). The upper bound of this unwanted contribution corresponds to R_{OC}. In order to circumvent such an effect and to allow for measurement with non-ideal sub-cells with less steep slopes (higher R_{OC}), we propose variable selective light biasing with the illumination intensity coupled to the electrical current flowing through the multi-junction. Also, for better control, instead of the usual approach of sourcing voltage and measuring current, we source current and measure voltage. The detailed algorithm for a tandem cell is as follows:

1) At the beginning, the tandem cell is illuminated by 1 sun, no current is sourced ($I=0$), and both sub-cells are in open circuit ($V_1=V_{OC,1}$, $V_2=V_{OC,2}$). The total voltage V_{sum}, equal to the sum of both V_{OC} values ($V_{sum}=V_{OC,1}+V_{OC,2}$), is registered on the tandem cell terminals.
2) While maintaining 1 sun illumination, a current ΔI is sourced onto the terminals and flows through the tandem cell. The working points of the sub-cells follow this sourced current. Two different cases have to be met for the sub-cells in order to realize the I–V separation. For the sub-cell for which we want to measure the I–V curve, no additional bias light is applied, so that its working point will follow its respective 1 sun illuminated I–V characteristic ($I_1=\Delta I$, $V_1=V_1(\Delta I)$) with $V_1(I)$ being the sub-cell I–V curve. For the sub-cell that we do not want to measure, additional bias light is applied which generates additional photocurrent ΔI_{ph} in this sub-cell. If this bias light is adjusted so that the additional photocurrent matches the sourced current ($\Delta I_{ph}=\Delta I$), and if we apply the shifting approximation (I and I_{ph} just superpose, but with opposite sign), then the sub-cell working point under the 1 sun and additional bias light illumination ($V_{2,bias}$, ΔI) is defined as $V_{2,bias}(\Delta I)=V_2(\Delta I-\Delta I_{ph})=V_{OC,2}$ with $V_2(I)$ and $V_{2,bias}(I)$ being the sub-cell I–V curves under 1 sun illumination and under 1 sun illumination plus light bias, respectively. Thus, by properly scaling the intensity of the selective light bias, the I–V curve of the non-evaluated sub-cell is "vertically" shifted so as to allow its working point to remain at a constant voltage ($V_{OC,2}$) for given sourced current ΔI (see Fig. 1).
3) Simultaneously, the voltage V_{sum} on the tandem cell terminals is measured. As the voltage on the light-biased sub-cell is fixed, a variation in the measured voltage corresponds only to a change in voltage on the unbiased sub-cell ($I=\Delta I$, $V_{sum}=V_1(\Delta I)+V_{OC,2}$).
4) Steps 2 and 3 are repeated for higher values of sourced current ΔI until the measured voltage drops to the $V_{OC,2}$ of the light-biased sub-cell.
5) Finally, $V_{OC,2}$ is subtracted from the measured curve and the component I–V curve of the unbiased sub-cell is obtained ($V_{sum}-V_{OC,2}=V_1(I)$). No assumption has to be made about this sub-cell because it is kept all the time under constant 1 sun illumination.

To analyze the method from a mathematical point of view, we start with the shifting approximation that, as we discussed in the introduction, is equivalent to formula (1) with the serial resistance neglected ($R_s=0$). Formula (3) is then its differential form. Formula (4) is obtained by setting $V=0$ to describe short-circuit conditions. Formulae (3) and (4) express now the shifting approximation in a different way:

$$dI \cong -dI_{ph}+\frac{dI_{dark}(V)}{dV}dV \tag{3}$$

$$I_{ph} \cong -I_{SC} \tag{4}$$

Now, if we set $dI=-dI_{ph}$ and assume that the first derivative $dI_{dark}(V)/dV$ is nonzero, we get $dV=0$, meaning that the voltage is indeed kept constant. So it is possible to fix the voltage in this way. In order to make $dI=-dI_{ph}$, we have to know the value of I_{ph}. We use formula (4) to approximate I_{ph} by the short-circuit current I_{SC} obtained by integration of the EQE as follows:

$$I_{SC}=eA\int EQE_{SC}(\lambda)\phi_{source}(\lambda)\,d\lambda \tag{5}$$

where EQE_{SC} is the EQE measured at short-circuit conditions, $\phi_{source}(\lambda)$ is the photon flux of the light bias, e is electron charge and A is active area. The error regarding the use of the shifting approximation is evaluated in Section 4.

2.2. Experimental setup

The experimental setup is schematically depicted in Fig. 2. A class AAA Wacom Super Solar Simulator was used to deliver standard test illumination of 1000 W/m^2 with an AM1.5 spectrum. A set of 15 focused blue LEDs ($\lambda=470$ nm, ø=5 mm, $\Theta=160$ mW/sr) was used for the top cell light bias and a set of 24 focused infrared LEDs ($\lambda=850$ nm, ø=5 mm, $\Theta=700$ mW/sr) was used for the bottom cell light bias. The two sets of LEDs were driven through a computer-controlled current source to illuminate homogeneously an area of 0.3 cm^2 defined by a mask. For the electrical measurements we employed a Keithley 236 source-measure unit. The LED intensities were calibrated by measuring the electrical current $I_{reference}$ of a reference photodiode with a calibrated EQE spectrum, placed below the mask. The relative LED spectra $\phi_{source,rel}(\lambda)$ were measured by a CCD spectrometer (see Fig. 3).

2.3. Test measurement

In order to test the new I–V separation method, a special three-terminal thin-film silicon device was fabricated. The test cell was an a-Si:H/µc-Si:H tandem solar cell making use of textured zinc oxide (ZnO) as front and back contacts. A 5 µm-thick doped ZnO interlayer was deposited between the top and bottom cells to act as a common contact to the n-type doped layer of the p–i–n top cell and to the p-type doped layer of the bottom cell, i.e. as an intermediate contact. Due to the thickness of the ZnO interlayer, the bottom cell received less illumination and thus significantly limited the total current (see Fig. 3). This test device allows for typical I–V measurements of the monolithic tandem cell as well as for individual measurements of each junction by direct contact through the ZnO interlayer.

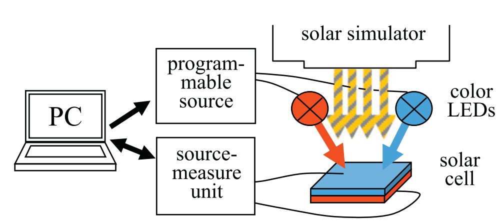

Fig. 2. Experimental setup of the new I–V separation method.

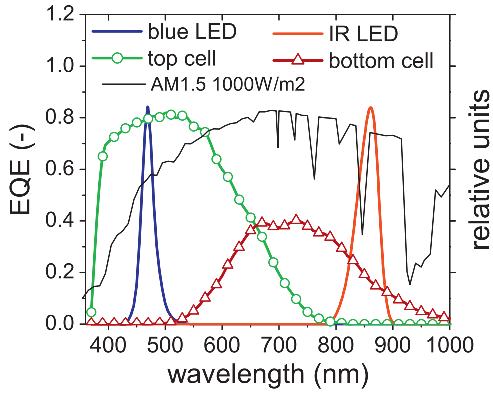

Fig. 3. Component *EQE* curves of the test cell and radiance spectra of the biasing LEDs (in relative units). The *EQE* of the bottom cell is low because of the thick intermediate reflector and absence of a back reflector in this experiment.

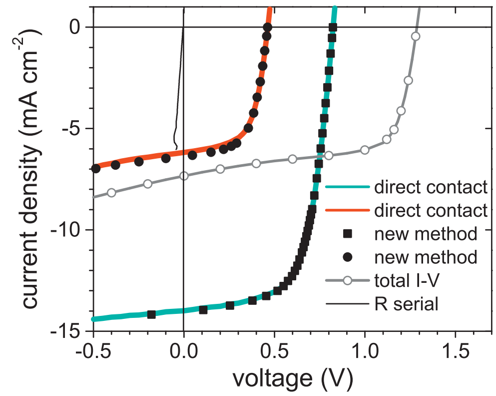

Fig. 4. Measured component *I–V* curves obtained with the new method (symbols) compared to direct measurement (thick solid colored lines). The total *I–V* curve is also shown (line with symbols) and the contribution of serial resistance (thin solid line). Current density was obtained by normalization of measured current to the illuminated area of 0.3 cm^2 (For interpretation of the references to color in this figure legend, the reader is referred to the web version of this article.).

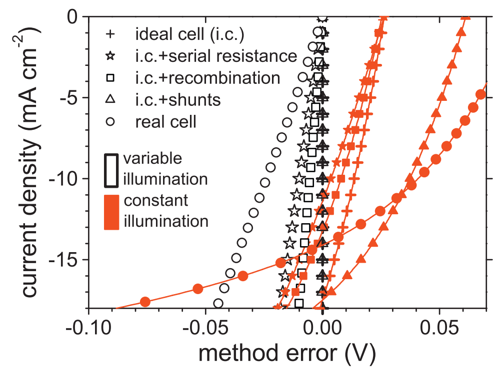

Fig. 5. Error in voltage domain given by the non-evaluated sub-cell as simulated for different input parameters and different methods: new variable illumination method—black empty symbols, constant illumination method—red lines with full symbols (For interpretation of the references to color in this figure legend, the reader is referred to the web version of this article.).

Before *I–V* measurement, quantum efficiency was measured on the test tandem cell to obtain the separate EQE spectra of the top and bottom cells [2]. Then the *I–V* measurement proceeded as follows: the side terminals of our test cell were connected to the source-measure unit, the sun simulator was switched on, and gradually increasing blue illumination was applied. At the same time, gradually increasing electrical current was sourced by the source-measure unit to the tandem cell and the voltage was recorded. The same procedure was repeated for the infrared illumination. For each sub-cell (top or bottom) and each illumination source (blue or IR LEDs), the level of current $I^{\text{source}}_{\text{sub-cell}}$ was calculated at each intensity step according to formula (6) using the values of the EQE spectrum of the given sub-cell, the corresponding value $I_{\text{reference}}$ obtained from calibration, and the relative LED spectrum of the given light-bias source $\phi_{\text{source,rel}}(\lambda)$. This formula is derived from applying formula (5) to the sub-cell and the reference detector:

$$I^{\text{source}}_{\text{sub-cell}} = \frac{\int EQE_{\text{sub-cell}}(\lambda)\ \phi_{\text{source, rel}}(\lambda)\ d\lambda}{\int EQE_{\text{reference}}(\lambda)\ \phi_{\text{source, rel}}(\lambda)\ d\lambda}\ I^{\text{source}}_{\text{reference}} \tag{6}$$

Finally the reference (true) *I–V* curves of the individual sub-cells were measured by using the direct contact to the ZnO interlayer. The lateral path of the current through the thick ZnO interlayer is short and the effect of the sheet resistance can be neglected.

3. Results

Fig. 4 shows a comparison between the component *I–V* curves of each sub-cell measured by the new technique described here and the reference *I–V* curves obtained by direct contact through the ZnO interlayer. In this case the input values of V_{OC}, necessary for subtracting the contribution from the biased sub-cell, were measured directly via the intermediate contact. The excellent agreement between the sub-cell's *I–V* characteristics directly measured and those obtained with the new technique demonstrates very good functionality of the presented concept even with non-ideal sub-cells. A near perfect match is obtained; small deviations are due to total serial resistance, which, as discussed in section 4, is added to both component *I–V* curves.

4. Discussion

In the previous discussions we were critical of methods that assume the shifting approximation. In our method, however, the shifting approximation is also assumed, but with a reduced effect because it concerns solely the steep region of the *I–V* curve of the non-evaluated sub-cell. The error introduced by the shifting approximation was therefore studied by numerical simulations of formula (1) including the recombination term (2). The simulations proceeded in several steps and reproduced the measurement procedure, depicted in Fig. 1.

1) The *I–V* curve of a typical single-junction a-Si:H solar cell illuminated by 1 sun was first simulated by the value of photogenerated current I_{ph} set to obtain a typical experimental value of I_{SC} at 1 sun. The operating point follows the sourced current and is at the open-circuit ($I=0$, $V=V_{OC}$) at the beginning.

2) The photogenerated current I_{ph} was adjusted to increase the value of current at the short circuit by a small step ΔI. Note that we do not rely on approximation (4) and so the value of I_{ph} is assumed to be unknown, as in the experiment.

3) A new position of operating point is located at $I=\Delta I$ and a new value of voltage is obtained ($V \rightarrow V_{OC}+\delta$). The difference δ then represents the voltage variation representing the error of the shifting approximation. The plots of the error δ with respect to driven current ΔI for several different cases are in Fig. 5. For comparison, the error of the constant illumination method is plotted too.

In these simulations we focused on the effect of the serial resistance R_s, of the shunt resistance R_{sh} and of the recombination parameter $(\mu\tau)_{\text{eff}}$ because these factors "complicate" the electrical behavior or lead to violations of the shifting approximation. For an "ideal cell" where all these values are in a range for which their effect is negligible ($R_s = 0\,\Omega\,\text{cm}^2$, $R_{sh} = 10\,\text{k}\Omega\,\text{cm}^2$ and $(\mu\tau)_{\text{eff}} = 10^{-5}\,\text{cm}^2\,\text{V}^{-1}$) we obtain for the new method a straight vertical line, meaning that the voltage on the cell is constant, that the shifting approximation holds and that no error arises (Fig. 5, crosses). Interestingly, no error is observed even when strong shunting ($R_{sh} = 60\,\Omega\,\text{cm}^2$) is considered, because if no serial resistance is present the effect of shunts will be represented only by a current-independent term (Fig. 5, triangles). However, the effect of shunts will appear if shunting is combined with serial resistance.

When only serial resistance is introduced ($R_s = 1\,\Omega\,\text{cm}^2$) the voltage contribution is no longer constant and a tilted line (Fig. 5, stars) is obtained because, as discussed in the introduction, the serial resistance invalidates the shifting approximation. The tilted line is added to the measured *I–V* as error. We found that the slope of the line corresponds exactly to the simulated value of serial resistance. This means that if the serial resistance is attributed to the light-biased (non-evaluated) sub-cell, its effect will nevertheless be added to the measured cell as if the serial resistance were in the measured cell. Indeed, if there is a serial resistance anywhere in the multi-junction cell, we cannot attribute it to one specific sub-cell, and therefore the effect of this "common" serial resistance will be always added to the evaluated sub-cell. In other words, in the case of a two-junction cell, the serial resistance is measured twice. Consequently, the sum of the two evaluated sub-cell *I–V* curves (in the voltage domain) will not give the total multi-junction cell *I–V* characteristic obtained by regular measurement. The difference will correspond to the effect of the serial resistance R_s, which can thus be evaluated according to formula (7), where V^{total} is regularly measured overall *I–V* curve of tandem cell. This is also indicated in Fig. 4. It is possible to go even further, correcting the resulting *I–V* curves with the known serial resistance to obtain "R_s-free" *I–V* curves.

$$V_{\text{topcell}}^{\text{component}} + V_{\text{bottomcell}}^{\text{component}} - V^{\text{total}} = IR_{\text{serial}} \tag{7}$$

The carrier recombination can be accounted for, for example, by taking a value for a light-soaked a-Si:H cell [14]: $(\mu\tau)_{\text{eff}} = 7.7 \times 10^{-9}\,\text{cm}^2\,\text{V}^{-1}$. As shown in Fig. 5 (squares) an effect similar to serial resistance is obtained, allowing us to represent the effect in terms of a serial resistance of $0.56\,\Omega\,\text{cm}^2$.

Including all three parasitic effects, we obtained a simulation of a "real cell" (Fig. 5, circles) which appears as a tilted line with an effective serial resistance of $2.05\,\Omega\,\text{cm}^2$. This actually expresses the error of the new method in the case of a real cell, meaning that the obtained *I–V* curve of the evaluated sub-cell differs from the true curve as if this additional serial resistance had been added. The comparison of the errors in the new method and the method of constant illumination clearly proves that the new method is much more accurate in all cases (see Fig. 5).

Moreover the new method is only weakly sensitive to inaccuracies in the quantities in formula (6), e.g. due to improper light or voltage bias during *EQE* measurement. Such additional error (in the voltage domain) depends on the value of R_{OC}, which is on the order of tens of $\Omega\,\text{cm}^2$. Thus an error of few tenths of mA cm^{-2} would translate into an error of a few mV in an *I–V* curve. Similarly, the method is only weakly sensitive to imperfections of illumination selectivity. Any unintended bias illumination of the non-selected sub-cell has to be on the same order as the intensity stability of the solar simulator.

To extend the presented procedure to multi-junction cells composed of a larger number of sub-cells, a light-biasing system that selectively illuminates each sub-cell is necessary. Then a series of measurements has to be done with different combinations of measured and light-biased sub-cells. In the simplest case, in each measurement only one sub-cell can be measured and the other sub-cells can be light biased to keep their voltage constant. However, since the measurement error comes from the light-biased cells only, this choice would lead to a large error given by the sum of errors from all light-biased sub-cells. On the other hand if only one sub-cell in each measurement is light-biased, the error is minimized. The latter choice, however, also requires solving a simple set of linear equations to get the individual *I–V* curves of the sub-cells.

5. Conclusions

A new method of measurement of component *I–V* curves based on variable selective light bias coupled to the level of current flowing through the device during the *I–V* measurement is shown. It represents a significant improvement compared to previously reported methods based on constant selective light bias. The strength of the approach lies in its ability to measure thin-film p–i–n cells with complex electrical behavior, including bulk recombination and strong shunts, and in the fact that no numerical model is necessary. The only input parameters are the quantum efficiency spectra and V_{OCs} of the individual sub-cells that can be obtained by an independent V_{OC} separation procedure [17]. By numerical simulations, the accuracy of the method was evaluated for various non-ideal devices. This method is robust and insensitive to typical errors or imperfections in illumination selectivity. The method was successfully tested on a dual-junction device, but can principally work as well on an arbitrary number of interconnected sub-cells provided individual selective illumination is possible.

Acknowledgment

This work was supported by the Swiss Federal Office of Energy (OFEN) Grant no. 101191, and by the Czech Science Foundation Project no. GA202/09/0417 and Grant no. SVV-2010-261306.

References

[1] J. Bailat, et al., Recent developments of high-efficiency micromorph tandem solar cells in KAI-M PECVD reactors, in: Proceedings of the 25th EU PVSEC/5th WCPEC, 6–10 September 2010, Valencia, Spain, pp. 2720–2723.
[2] J. Burdick, T. Glatfelter, Spectral response and *I–V* measurements of tandem amorphous-silicon alloy solar cells, Solar Cells 18 (1986) 301–314.
[3] S. Kurtz, K. Emery, J.M. Olson, Methods for analysis of two-junction two-terminal photovoltaic device, in: Proceedings of the 1st WCPEC, 1994, pp. 1733–1737.
[4] C. Das, X. Xiang, X. Deng, Method for measuring component cell current–voltage characteristics in a multi-junction, two-terminal stacked solar cell, High Efficiency and High Rate Deposited Amorphous Silicon-Based Solar Cells, National Renewable Energy Laboratory, University of Toledo, Toledo, 2006 OH, Rep. NREL/SR-520-39091 pp. 73–80.
[5] Y. Tsuno, Y. Hishikawa, K. Kurokawa, Separation of the *I–V* curve of each component cell of multijunction solar cells, in: Conference Record of the 31st IEEE Photovoltaic Specialists Conference, 2005, pp. 1476–1479.
[6] R. Adelhelrn, K. Bücher, Performance and parameter analysis of tandem solar cells using measurements at multiple spectral conditions, Solar Energy Materials and Solar Cells 50 (1998) 185–195.
[7] J. Holovský, M. Vaněček, Non-destructive technique to measurement and separation of *I–V* curves of monolithic multi-junction solar cells, in: Proceedings of the 24th EUPVSEC, 2009,Hamburg, Germany, pp. 2757–2759.
[8] B. Chhabra, S. Jacobs, C.B. Honsberg, Suns–V_{OC} and minority carrier lifetime measurements of III–V tandem solar cells, in: Proceedings of the IEEE 4th World Conference on Photovoltaic Energy Conversion, 2006, Waikoloa, HI, USA, pp. 791–794.
[9] S.H. Lim, et al., Analysis of spectral photocurrent response from multi-junction solar cells under variable voltage bias, in: Proceedings of the 35th IEEE Photovoltaic Specialists Conference (PVSC), 20–25 June 2010,Honolulu, HI, USA, doi: 10.1109/PVSC.2010.5617046.

[10] F.A. Lindholm, J.G. Fossum, E.L. Burgess, Application of the superposition principle to solar-cell analysis, IEEE Transactions on Electronics Devices 3 (1979) 165–171. (ED-26).
[11] M. Wolf, H. Rauschenbach, Series resistance effects on solar cell measurements, in: Advanced Energy Conversion, vol. 3, Pergamon Press, 1963, pp. 455–479.
[12] S.J. Robinson, A.G. Aberle, M.A. Green, Departures from the principle of superposition in silicon solar cells, Journal of Applied Physics 76 (12) (1994) 7920–7930.
[13] Y. Hishikawa, S. Okamoto, Dependence of the *I–V* characteristics of amorphous silicon solar cells on illumination intensity and temperature, Solar Energy Materials and Solar Cells 33 (1994) 157–168.
[14] J. Merten, et al., Improved equivalent circuit and analytical model for amorphous silicon solar cells and modules, IEEE Transactions on Electronic Devices 45 (1998) 423–429.
[15] R.A. Sinton, A. Cuevas, A quasi-steady-state open-circuit voltage method for solar cell characterization, in: Proceedings of the 16th European Photovoltaic Solar Energy Conference, 1–5 May 2000, Glasgow, UK , pp. 1152–1155.
[16] A.G. Aberle, S.R. Wenham, M.A. Green, A new method for accurate measurements of the lumped series resistance of solar cells, in: Conference Record of the 23rd IEEE Photovoltaic Specialists Conference, Louisville, 10–14 May 1993, KY, USA, pp. 133–139, doi: 10.1109/PVSC.1993.347065.
[17] J. Holovský, et al., Measurement of the open circuit voltage of individual subcells in a dual-junction solar cell, IEEE Journal of Photovoltaics 2 (2012) 164–168.